

Supplementary Materials for

Particle-based artificial three-dimensional stem cell spheroids for revascularization of ischemic diseases

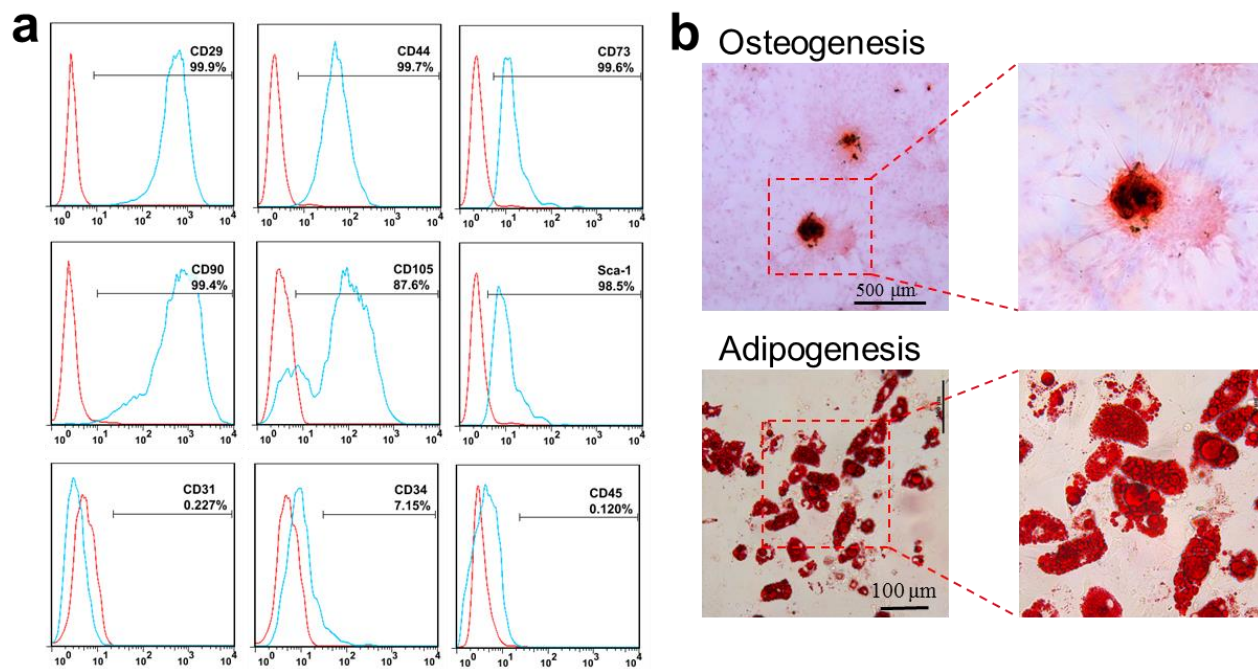
Ran Zhang, Wenya Luo, Yue Zhang, Dashuai Zhu, Adam C. Midgley, Hao Song, Anila Khalique, Haoqi Zhang, Jie Zhuang, Deling Kong*, Xinglu Huang*

*Corresponding author. Email: huangxinglu@nankai.edu.cn (X.H.); kongdeling@nankai.edu.cn (D.K.)

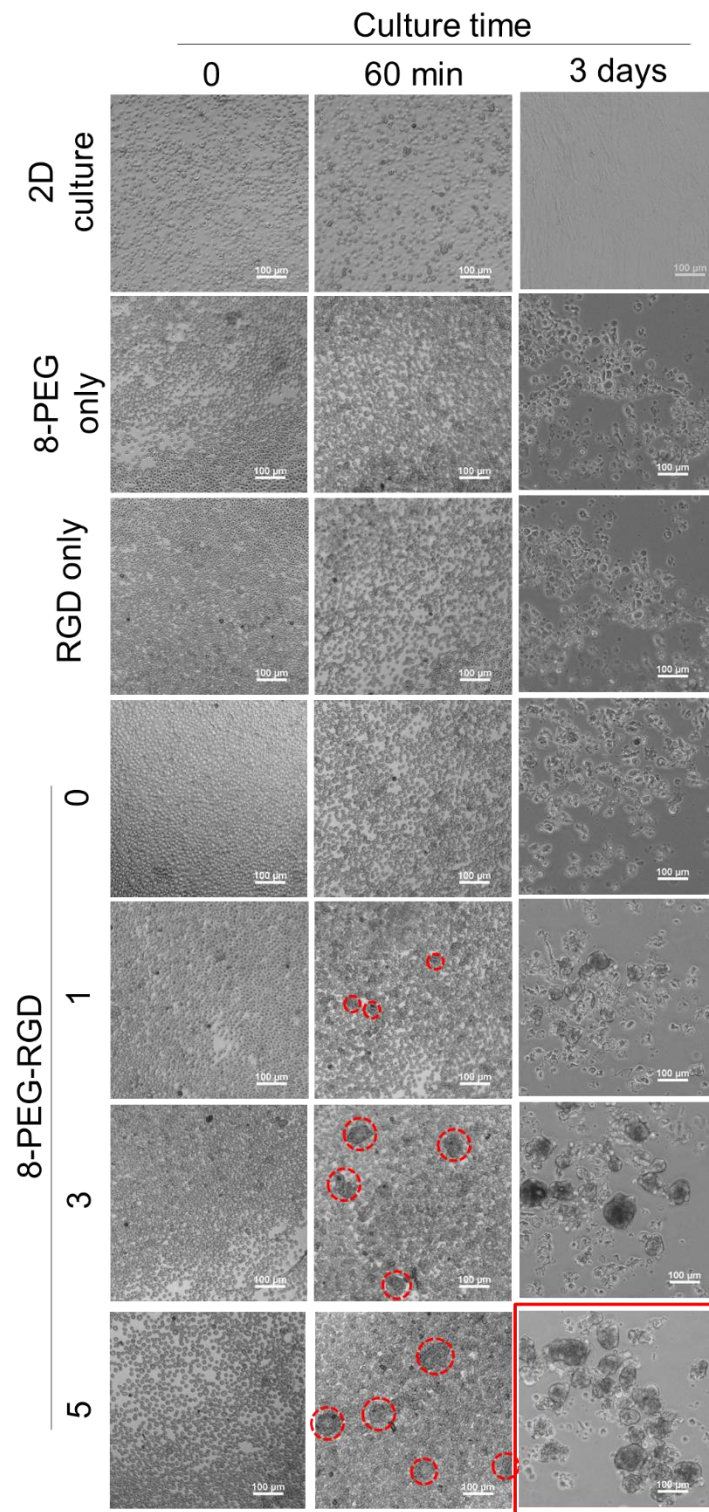
Published 6 May 2020, *Sci. Adv.* **6**, eaaz8011 (2020)
DOI: 10.1126/sciadv.aaz8011

This PDF file includes:

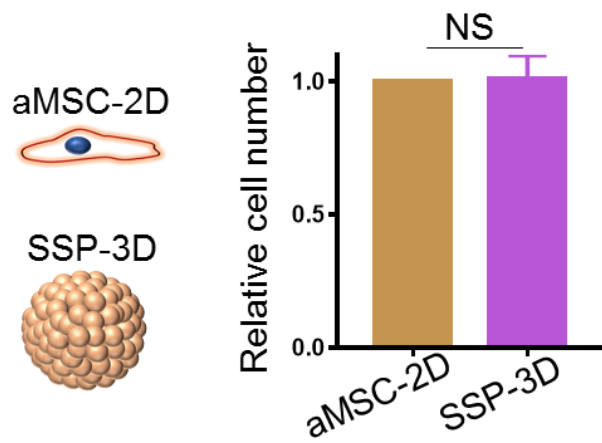
Figs. S1 to S9
Table S1



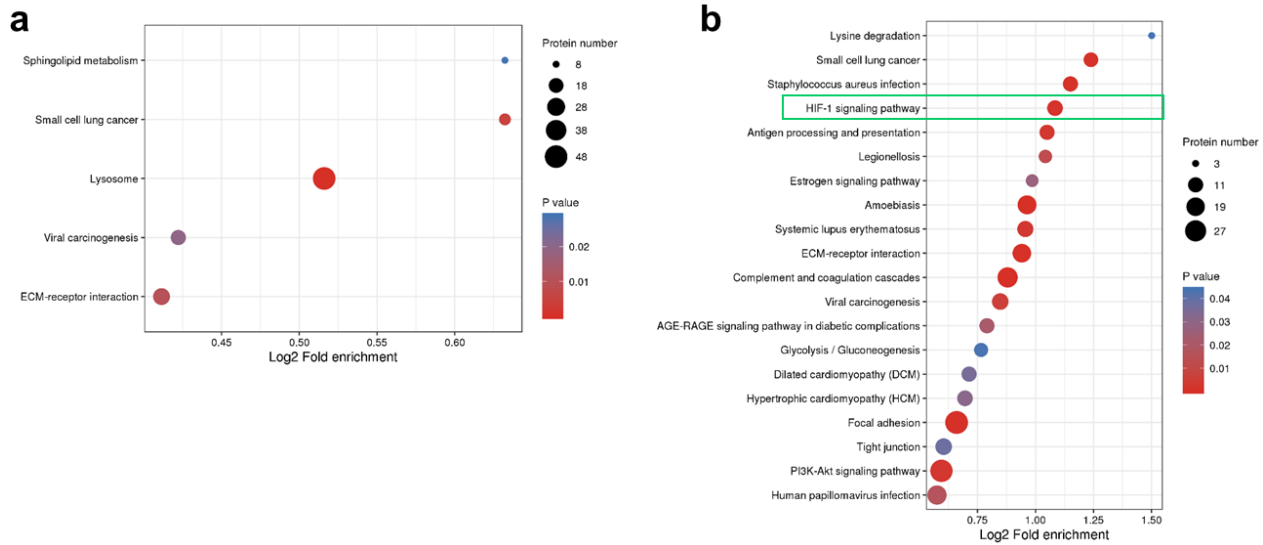
Supplementary Fig. 1. Characterization of aMSC. (a) Typical negative and positive surface marker expression in aMSC, as assessed by flow cytometry analysis. (b) Differentiation of aMSC into osteogenesis and adipogenesis using specific differentiation medium culture.



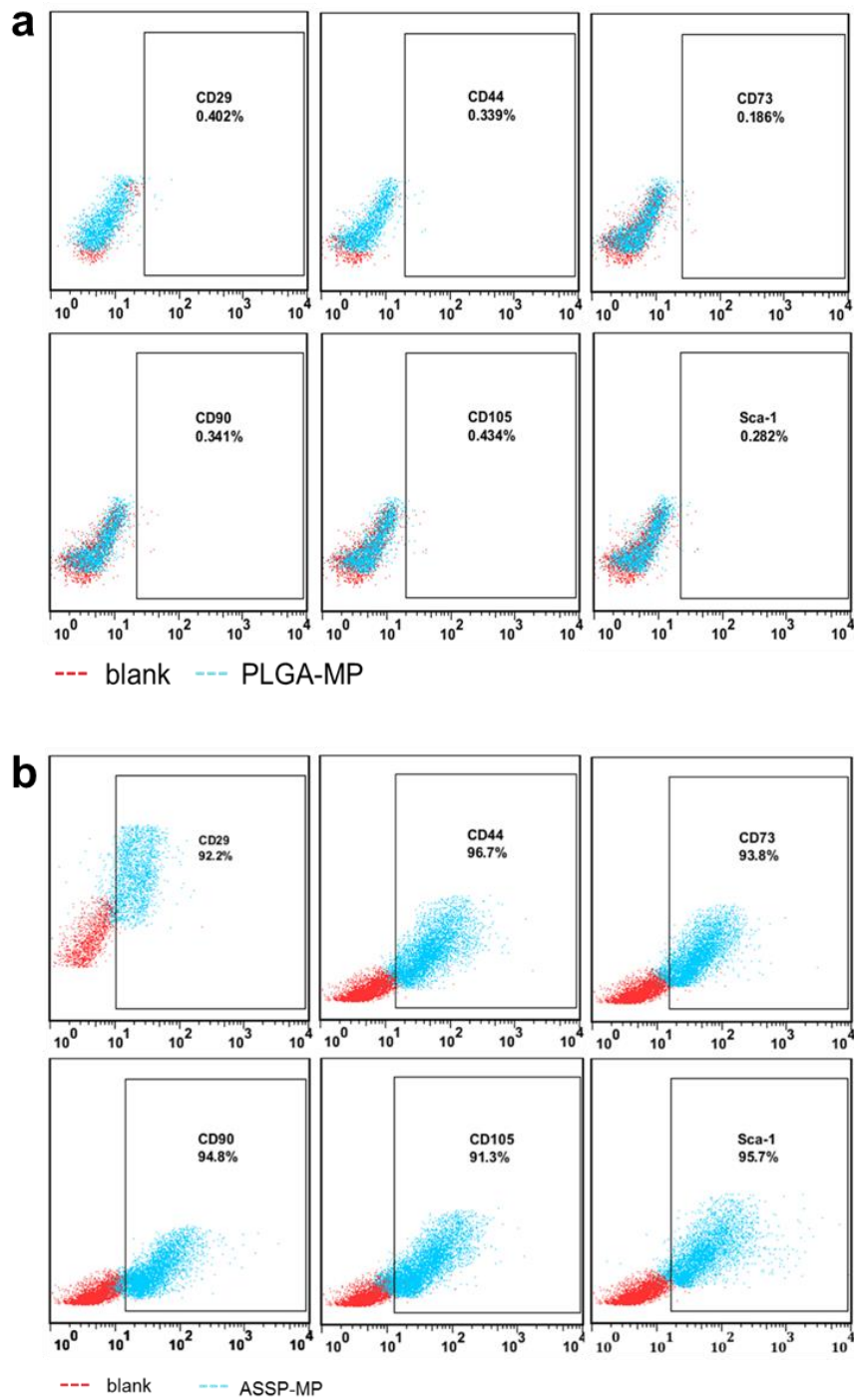
Supplementary Fig. 2. Optimization of the formation of 3D SSPs. Representative images of the formation of 3D SSPs in different treatments under microscopy observation.



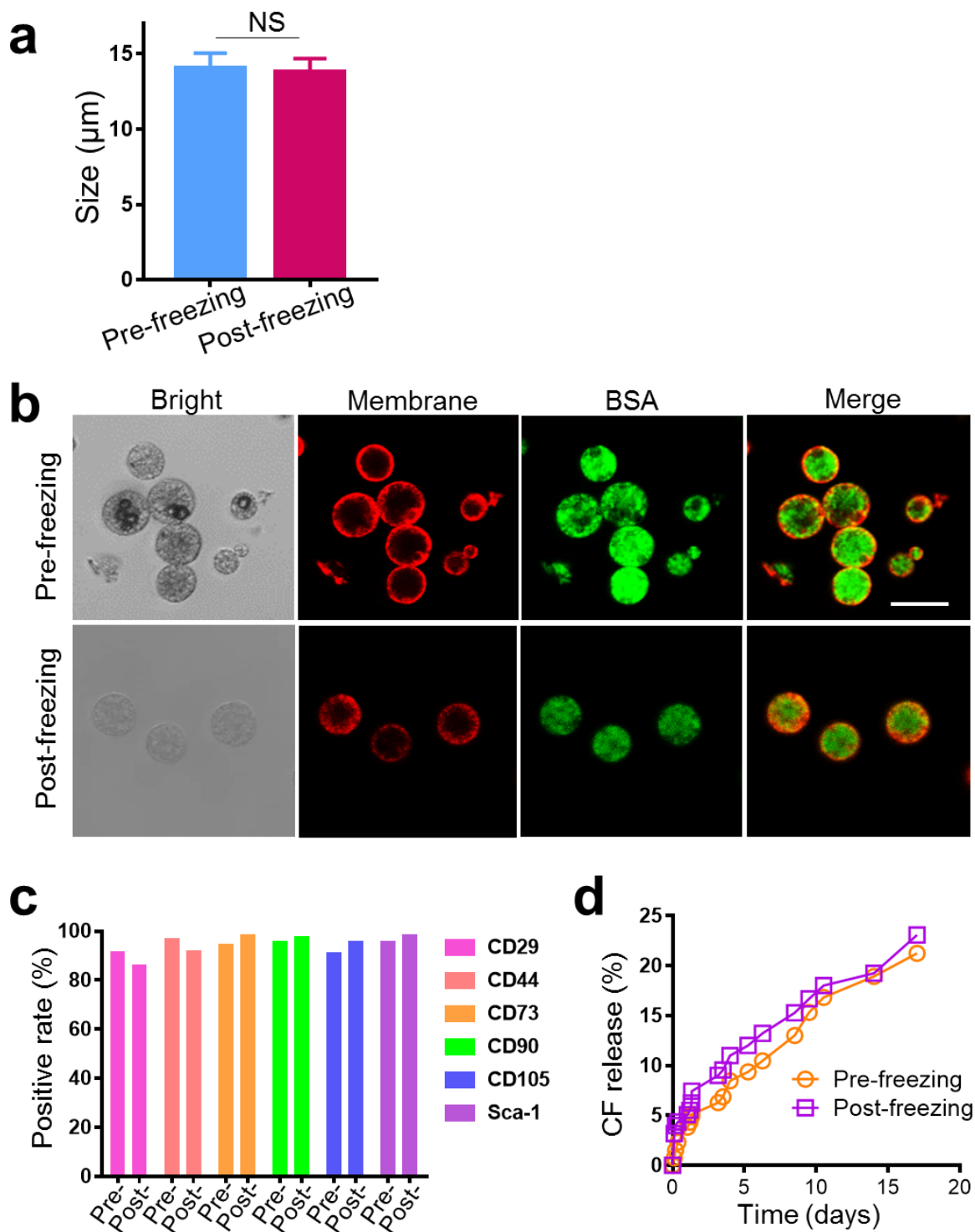
Supplementary Fig. 3. Comparison of cell number of 2D-aMSC and 3D SSP at 5 days after culture in serum-free medium. All data are presented as means \pm SEM. A two-tailed, unpaired Student's t test was used to compare between any two groups.



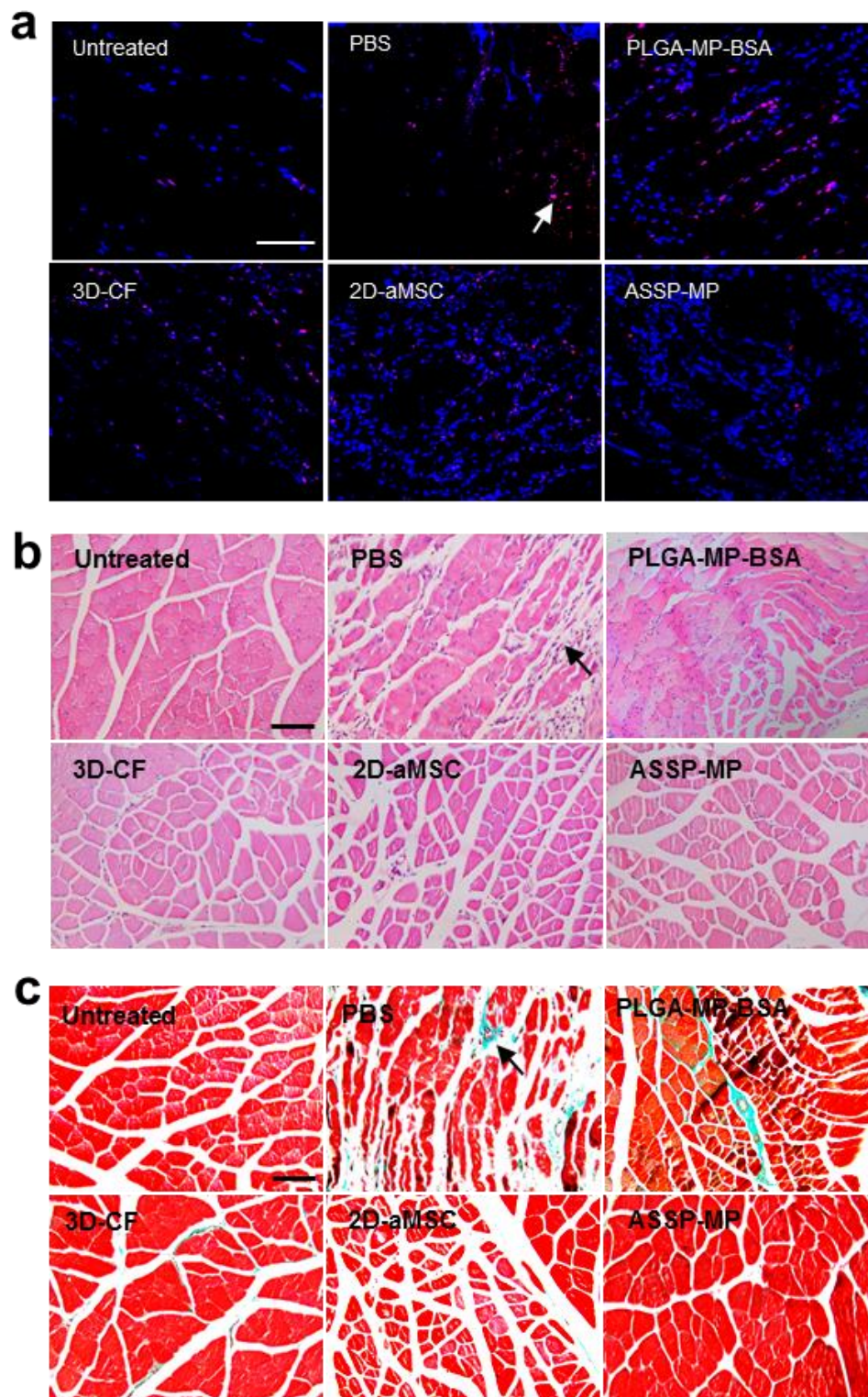
Supplementary Fig. 4. Comparison between 2D-CF and 3D-CF by KEGG pathway based on LC-MS proteomic analysis. The unsupervised enrichment analysis of KEGG pathway in (a) 2D-CF and (b) 3D-CF, respectively.



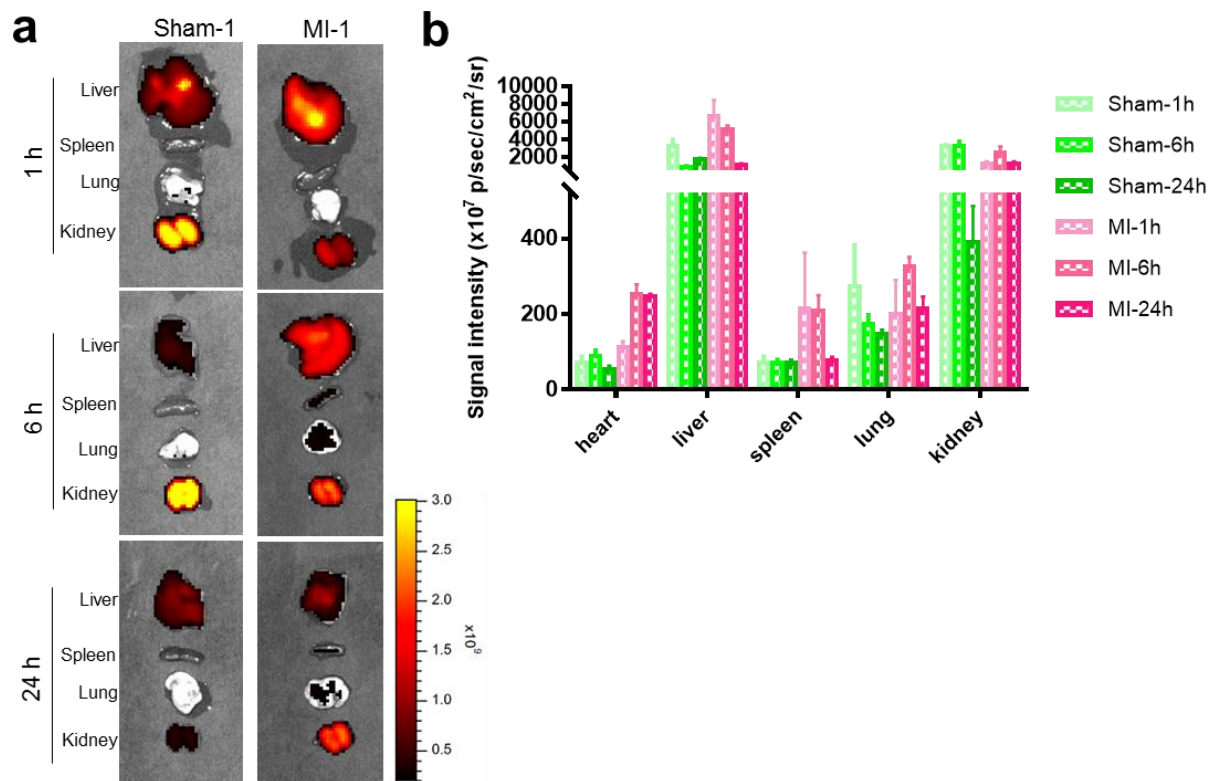
Supplementary Fig. 5. Flow cytometry analysis of surface markers on the MP without or with membrane coating. (a) Negative and (b) positive expression on PLGA-MP and ASSP-MP surface based on different surface markers analysis, respectively.



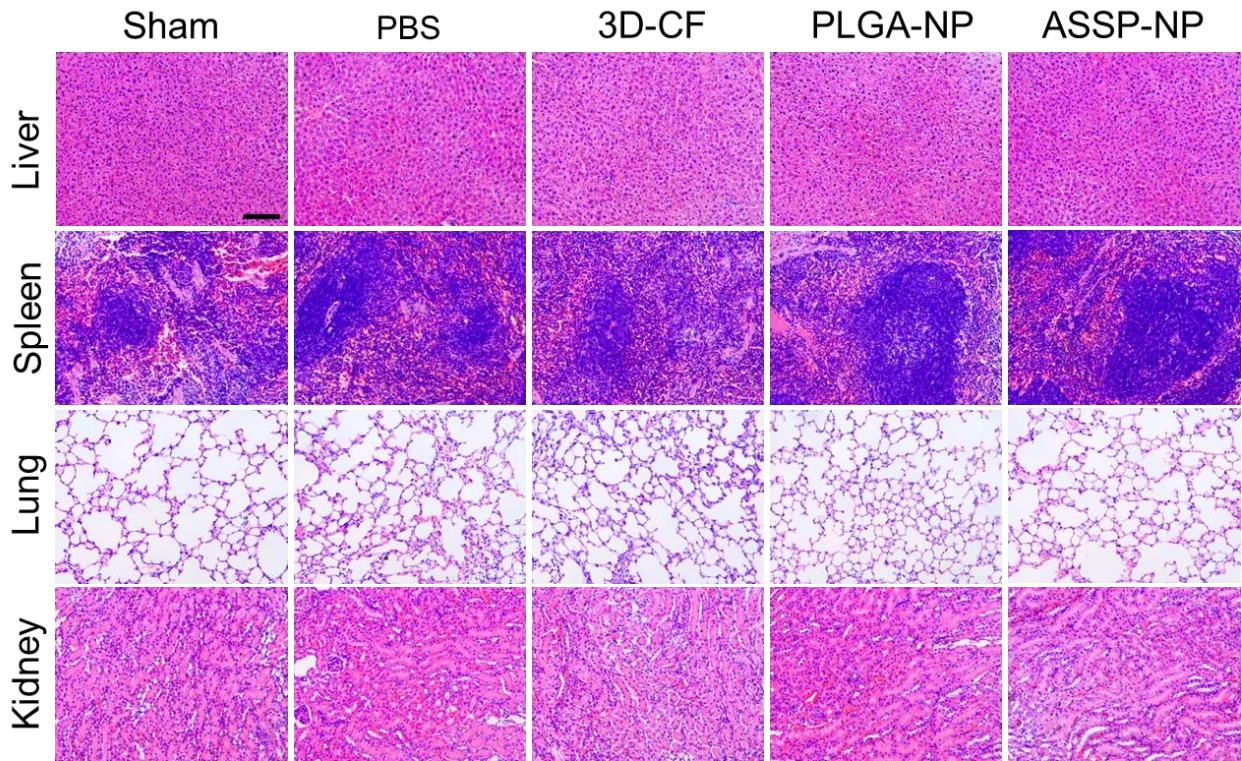
Supplementary Fig. 6. Characterization of ASSPs before and after cryo-storage. (a) Mean diameter of ASSP before and after freezing. (b) Confocal imaging of membrane structure in pre- and post-freezing samples, demonstrating cryopreservation does not affect membrane coating. Scale bar = 20 µm. (c) Surface marker expression of ASSP before and after freezing using flow cytometry analysis. (d) CF release kinetics from pre- and post-freezing samples. All data are presented as means \pm SEM. A two-tailed, unpaired Student's t test was used to compare between any two groups.



Supplementary Fig. 7. Histological analysis of the isolated muscles from the mice subjected to acute HI model. (a) Representative images of the apoptosis (arrow) of the samples by TUNEL immunostaining assay. Scale bar = 100 μm. (b) H&E staining of inflammation infiltration tissue (arrow) without or with different treatments. Scale bar = 100 μm. (c) Masson's Trichrome staining analysis of the fibrosis (arrow) in isolated muscles. Scale bar = 100 μm.



Supplementary Fig. 8. Biodistribution of ASSP-NP following i.v. administration. (a) IVIS fluorescence imaging and (b) quantification analysis of ASSP-NP in different organs at the indicated time points.



Supplementary Fig. 9. Histopathological analysis of systemic toxicities in different organs. The major organs without or with different treatments were harvested and assessed by H&E staining for variances in tissue architecture. Scale bar = 100 μ m.

Table S1. The sequences of primers for pro-angiogenic factors

| | Prime sequences |
|-------|--|
| VEGF | Forward: ACTGGACCCTGGCTTTAC Reverse: TCTGCTCTCCTTCTGTCGTG |
| PLGF | Forward: CTTCTGAGTCGCTGTAGTGG Reverse: TCCTTTCTGCCTTTGTCG |
| IGF | Forward: TGGATGCTCTTCAGTTCGTG Reverse: GTCTTGGGCATGTCAGTGTG |
| Ang-1 | Forward: ACAGGGACAGCAGGCAAAC Reverse: GGCATCGAACCACCAACC |
| PDGF | Forward: ATCCAGGGAGCAGCGAGCCA Reverse: CAGGGCCGCCTTGTCATGGG |
| EGF | Forward: GAGCCACCCTCATAATCACA Reverse: CCCGAGTTCTTCTAAGTTCCT |
| GADPH | Forward: TTGTCTCCTGCGACTTCAAC Reverse: GTCATACCAGGAAATGAGCTTG |